

Safety Verification of Seismic Isolation System using Oil and Viscous Dampers against Long Period Earthquake Motions

S. Minewaki, M. Yamamoto & H. Yoneda

Research and Development Institute, Takenaka Corporation, Chiba, Japan

R. Maseki, I. Nagashima, & A. Nii

Technology Center, Taisei Corporation, Kanagawa, Japan

M. Takayama

Fukuoka University, Fukuoka, Japan

M. Kikuchi

Hokkaido University, Hokkaido, Japan

M. Iiba

Building Research Institute, Ibaraki, Japan



SUMMARY

Long period earthquake motions with large amplitudes are expected to occur in Japan in the near future and they may have a considerable impact on seismic isolated buildings. Therefore, it is important to verify the safety of such buildings against long period earthquake motions. This paper describes multi-cyclic loading tests of oil and viscous fluid dampers. The dampers investigated here have an energy absorption capacity to sustain at least 2 times of long period earthquake motion. The oil dampers showed almost no change in their loop shapes that relate damping force to displacement, and no oil leaking was observed, although oil temperature exceeded the allowable value. The viscous fluid dampers showed a continuous decline in their damping force through the cyclic loading. After the temperature of viscous fluid fell enough, the initial dynamic characteristics were recovered. A new evaluation formula for declination of damping force was proposed.

Keywords: Seismic isolation, Long period earthquake motions, Oil damper, Viscous fluid damper

1. INTRODUCTION

In recent years, long period earthquake motions caused by subduction zone earthquakes around Japan as well as their impact on super high-rise buildings and base-isolated buildings have attracted great public concern and interest within the country. In fact, the 2011 off the Pacific coast of Tohoku Earthquake induced long period earthquake motions in the Kanto plain, which shook super high-rise buildings as well as base-isolated buildings for a long duration lasting more than several minutes. The Tokai, Tonankai, Nankai earthquakes or their coupled actions may occur in the near future and the Kanto, Nobi and Osaka plains will be exposed to long period earthquake motions with large amplitudes. It is therefore very important and essential to verify the safety of seismic isolation system against long period earthquake motions.

For that purpose, multi-cyclic loading tests were conducted on oil and viscous fluid dampers used for seismic isolated buildings.

2. TESTS OF OIL DAMPER

2.1. Objective

Although the existing knowledge about the basic characteristic of oil dampers had been reported by Japan Society of Seismic Isolation (2010) and Suzuki et al. (2008), etc. , the scope of that for the limit

state is limited at present. While leakage of oil from seal, caused by temperature rise, is considered as the limit state of such dampers, their response against long period earthquake motion is still not well evaluated. The objective of the multi-cyclic loading test described here is to extend the scope of knowledge for the limit state of oil dampers.

2.2. Specimens

Three specimens with different characteristics are used for the test. All of them are uni-flow type oil dampers made for seismic isolated buildings. The maximum damping-force of every specimen is 1000kN and the oil seal is made of fluoro-resin. All the specimens have almost the same appearance like the one shown in Fig. 2.1. Table 2.1 lists the specifications of the specimens. The main difference of these three specimens is in the 1st coefficient of damping. Specimen 1 has bi-linear type damping characteristics. It is regarded as a standard type in this investigation, since it has been used mainly in recent years. Specimen 2 has linear type damping characteristics, and its 1st coefficient of damping is smaller than that of Specimen 1. Specimen 3 is a bi-linear type oil damper, and has the largest 1st coefficient of damping among all. The first two specimens are product types verified by Ministry of Land, Infrastructure, Transport and Tourism of Japan. The last specimen is specially manufactured for this test.



Figure 2.1. Appearance of the oil damper

Table 2.1. Specifications of Oil Damper Specimens

	Specimen 1	Specimen 2	Specimen 3
Product type	BM250-4C	BM250-6C	specially manufactured
Damping characteristics	bi-linear	linear	bi-linear
1st coefficient of damping	2.50 MN·s/m	0.80 MN·s/m	3.75 MN·s/m
2nd coefficient of damping	0.1695 MN·s/m		0.1695 MN·s/m
Relief velocity	0.32 m/s		0.208 m/s
Maximum velocity	1.5 m/s	1.25 m/s	1.5 m/s
Maximum damping force	1000 kN	1000 kN	1000 kN
Stroke	±700 mm	±700 mm	±700 mm

2.3. Test Conditions

Uni-axial dynamic loading machine was used for the test where loading was controlled by displacement. Table 2.2 shows the test conditions.

The test condition for the multi-cyclic loading was determined as the total amount of displacement of the damper might exceed 100m. This amount corresponded to twice or three times the response displacement that might be induced by one long period earthquake motion. Since the capability of the accumulator of the loading machine was not enough, the multi-cyclic loading test was divided into 21 segments. Loading interval for filling the accumulator was inserted between each segment. The length of the interval was about 5 minutes. Each segment had a starting part where the amplitude increased gradually, 6 cycles of sinusoidal wave with amplitude of 200mm and an ending part where the amplitude was decrease gradually. So, including the starting parts and the ending parts of each segment, the total amount of displacement might be said to be 151.2m. In order to examine whether the maximum damping force changed from the initial value, the basic performance test was carried out when the multi-cyclic loading test was done and when oil temperature fell low enough. Besides the

damping force and displacement, temperature of the damper was measured at the points shown in Fig.2.2.

Table 2.2. Test Conditions for Oil Dampers

	Loading wave	Period (s)	Displacement (mm)	Velocity (m/s)	Number of cycles	Number of segments	Total amount of displacement (m)
Multi-cyclic test	sinusoidal	4	200	0.314	126	21	100.8 [†]
Basic performance test	sinusoidal	4	95	0.15	2		
		4	159	0.25	2		
		4	318	0.5	2		
		2.22	354	1	2		

[†]starting and ending parts are not included

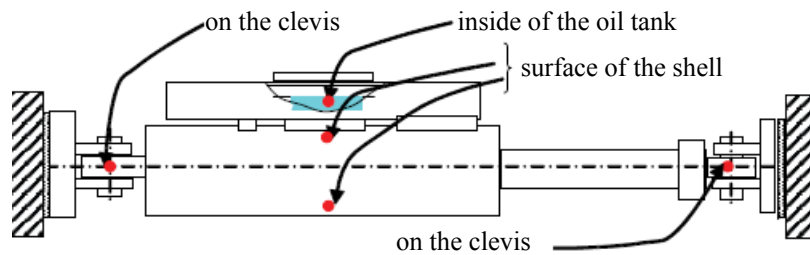


Figure 2.2. Measuring points of temperature

2.4. Test Results

The relations between damping force and displacement of specimen 1 and specimen 3 obtained by the multi-cyclic loading test are shown in Fig. 2.3. The relations between oil temperature rise and total displacement for each specimen are shown in Fig. 2.4. The relations between the temperature rise and absorbed energy are shown in Fig. 2.5. As shown in Fig. 2.4 and 2.5, the amounts of oil temperature rise for each specimens 1, 2 and 3 were, respectively, 73 °C, 26 °C and 83 °C, while the highest temperatures were 88 °C, 41 °C and 102 °C, respectively. As Shimizu Corporation et al. (2010) reported, the allowable maximum oil temperature in oil damper has been restricted to 80 °C. Although the result of specimen 1 and specimen 3 exceeded this value, either obvious changes in the shape of the damping force-displacement loops or leaking of oil out from the seal were not observed. The absorbed energy and the temperature rise in the oil are well correlated.

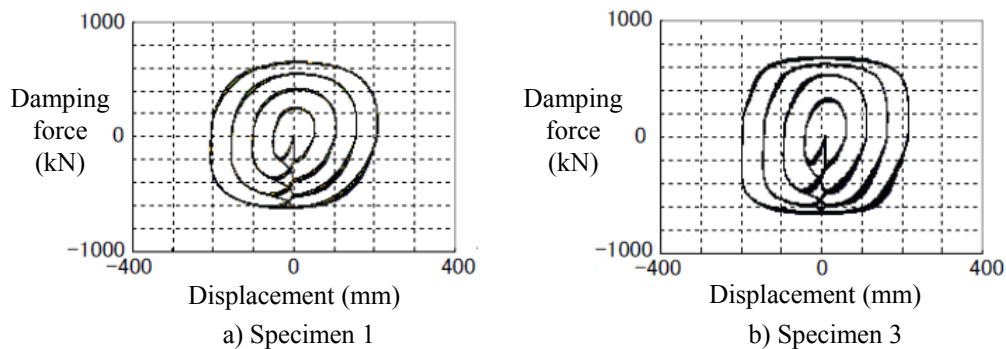


Figure 2.3. Relations between damping force and displacement

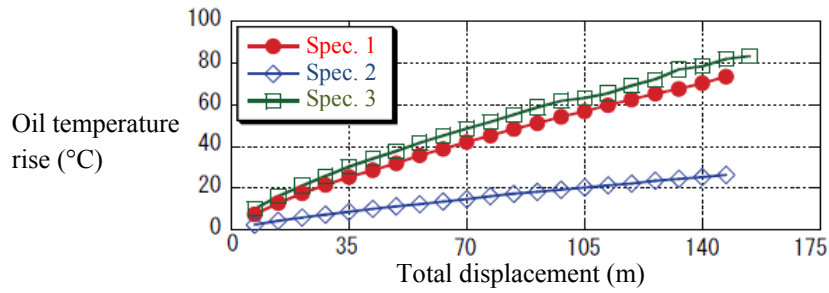


Figure 2.4. Relations between oil temperature rise and total displacement

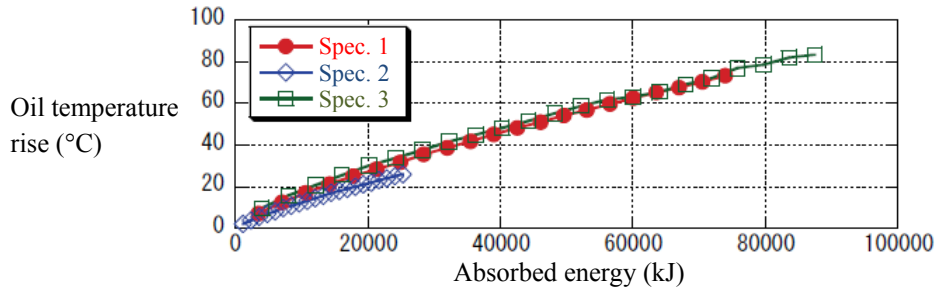


Figure 2.5. Relations between oil temperature rise and absorbed energy

Fig. 2.6 shows a comparison of experimental and calculated values of oil temperature rise. The calculated values were obtained by dividing the absorbed energy during the test by heat capacity of both the oil and steel in contact with oil, with/without considering heat transfer into the air. Temperature fall by heat transfer was calculated to be about 11 °C. When the intervals like those of this test were applied, although the calculated value without considering heat transfer gives fair approximation, considering heat transfer gives higher precision.

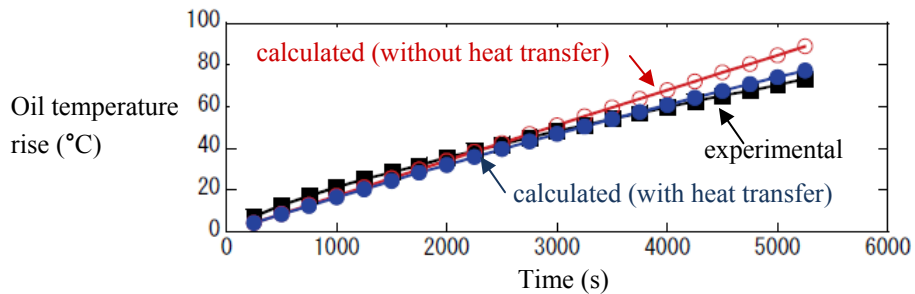


Figure 2.6. Calculated values of oil temperature rise

Fig. 2.7 shows relations between oil temperature and damping force for all specimens. Fig. 2.8 shows the relations between oil temperature and absorbed energy. The values of both figures were ratio relative to the value of 20 °C. The values of Fig. 2.7 were the maximum values extracted from each cycle, when the rod moved forward. With temperature rise, both the damping force and absorbed energy fell slightly. The ratios of the damping force at 100 °C were 0.97 when damper rod moved forward and 0.95 when damper rod moved backward (not shown on the figure). The ratio of the absorbed energy at 100 °C was 0.95.

Fig. 2.9 shows fluctuation of damping force obtained from the basic performance tests. These values were ratio relative to the initial damping force. Even immediately after the multi-cyclic loading test, when oil temperature was high, the values of ratio were not less than 0.94. After temperature fell down, the values seemed to be similar to the initial value.

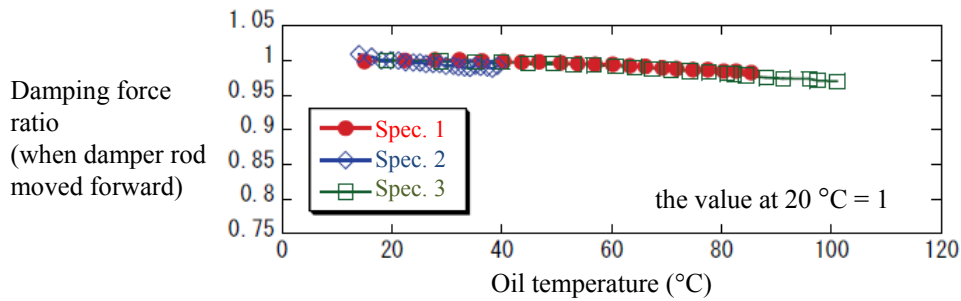


Figure 2.7. Relations between oil temperature and damping force

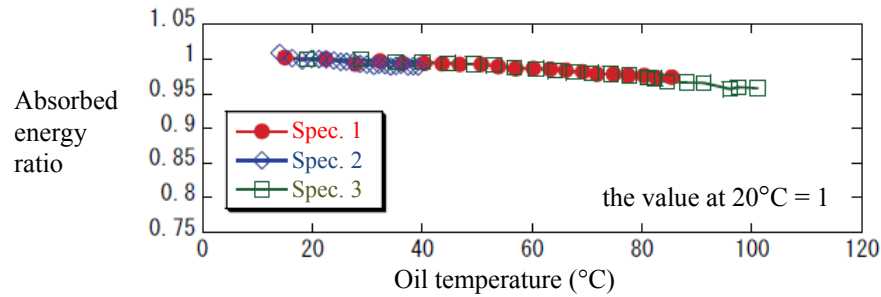


Figure 2.8. Relations between oil temperature and absorbed energy

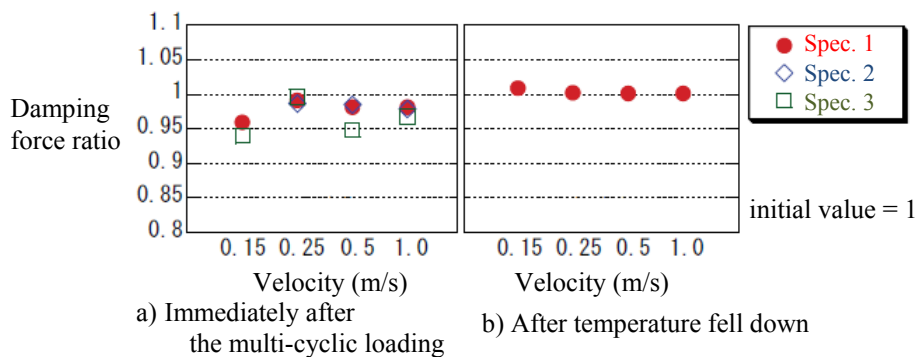


Figure 2.9. Damping force during the basic performance tests

3. TESTS OF VISCOUS FLUID DAMPER

3.1. Objective

The outline in Fig. 3.1 shows the composition of viscous fluid dampers. The feature of this type of dampers is in its ability to provide large damping force by changing axial movement produced by response of building into rotational movement. In verifications for base-isolated devices by Japan Ministry of Land, Infrastructure, Transport and Tourism (2004/2008) related to this type of dampers, conventional knowledge about such dampers' characteristics had been used. While it is already known that damping characteristics of these dampers are influenced by axial velocity and absorbed energy, the scope of the conventional knowledge was not enough to evaluate their response against long period earthquake motion. The objective of the multi-cyclic loading test described here is to extend the scope of knowledge for fluctuation in characteristics of such dampers.

3.2. Specimens

Three specimens were used in this test. Each of them respectively represents a type of the verification, i.e. number MVBR-0387, 0221 and 0222. The main difference of these types of verification was the

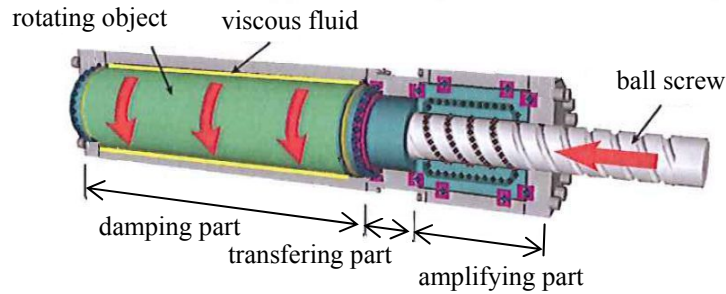


Figure 3.1. Composition of viscous fluid damper (Product type: 100000 cst and 300000 cst)

range of damping force capacity. Actually the capacities of specimens in this test were chosen based on the capability of the testing machine. Table 3.1 and Table 3.2 list the specifications of the specimens and testing machine capability, respectively.

Table 3.1. Specifications of Viscous Fluid Damper Specimens

Identification	RDT8	RDT16	RDT30
Product type	RDT-AT-Short	RDT-AT-100000cst	RDT-AT-300000cst
Verification number	MVBR-0387	MVBR-0221	MVBR-0222
Total length	1317mm	1756mm	1990mm
Stroke	±500 mm	±500 mm	±750 mm
Amplifying ratio	8.48	9.30	15.3
Maximum velocity	1.5 m/s	1.5 m/s	1.5 m/s
Maximum Damping force	80.2 kN	159.6 kN	299.0 kN

Table 3.2. Testing Machine Capability

Maximum Load	±300.0 kN
Stroke	±400 mm
Maximum velocity	0.5 m/s

3.3. Test Conditions

In this investigation, the total displacement of isolated layer against one long period earthquake motion was assumed 50 meters. The loading relative to this displacement was called a “set”. The displacement amplitude was selected as a test parameter where three levels were fixed. Three sets of each level were applied on each specimen when ultimate limit state did not appear. Intervals with length of about 10 minutes were inserted after every set for filling the accumulator of testing machine. Before testing on any level, temperature of all portions of the specimen was lowered enough. Basic performance tests were done before and after loading each level as well. The test conditions are listed in Table 3.3.

Table 3.3. Test Conditions for Viscous Fluid Dampers

	Level	Loading wave	Period (s)	Displacement (mm)	Number of cycles	Total amount of displacement (m)	Time of intervals (min.)	Number of sets
Multi-cyclic test	0	sinusoidal	4	200	63 [†]	50.4 [†]	10	3 ^{†††}
	1			300	42 [†]	50.4 [†]		
	2			100	125 [†]	50.0 [†]		
Basic performance test		sinusoidal	2	63.7	5 ^{††}			

[†]per one set, ^{††}starting part and ending part are included, ^{†††}when ultimate limit state did not appear

3.4. Test Results

Typical results of the multi-cyclic loading test are shown in Figs. 3.2 to 3.5 in terms of the damping force Q , temperature of the viscous fluid T and pressure inside the damper P . The results for level 0 of RDT30, level 1 of RDT30, level 1 of RDT16 and level 1 of RDT8 are presented with the figures' order. P or pressure inside the damper was not measured for RDT8. All the values used in the figures were measured when the displacement had become 0.

As a general tendency, while damping force declined monotonously, both temperature of the viscous fluid and pressure inside the damper rose monotonously. In spite of the existence of intervals, changes in the measurements described above are almost continuous, except for first some cycles of each set. The energy absorption performance, that is the basic function of damping devices, was not lost in almost all specimens and levels, except for 3rd set for level 1 of RDT8.

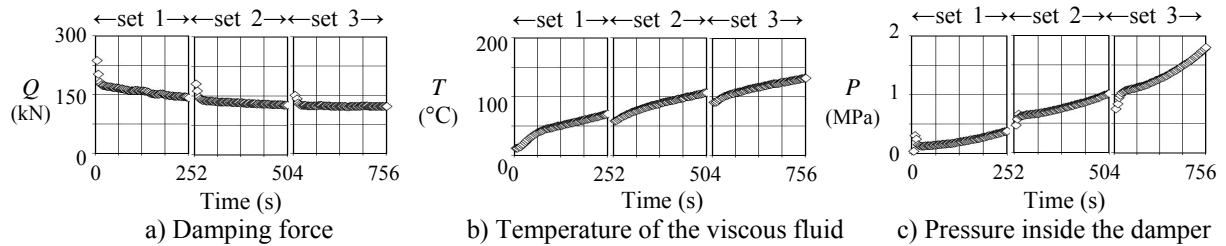


Figure 3.2. Result of multi-cyclic test for level 0 of RDT30

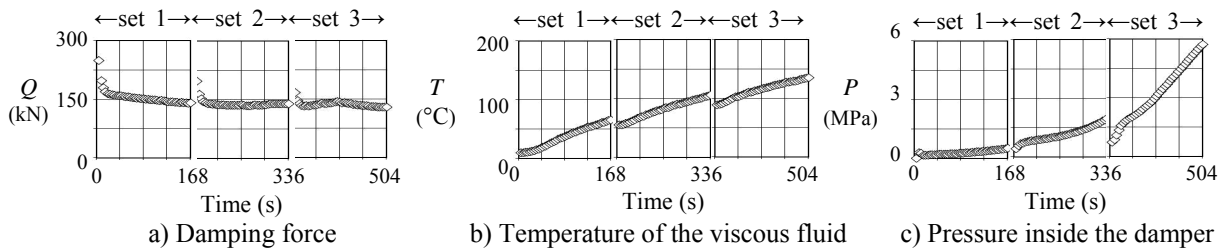


Figure 3.3. Result of multi-cyclic test for level 1 of RDT30

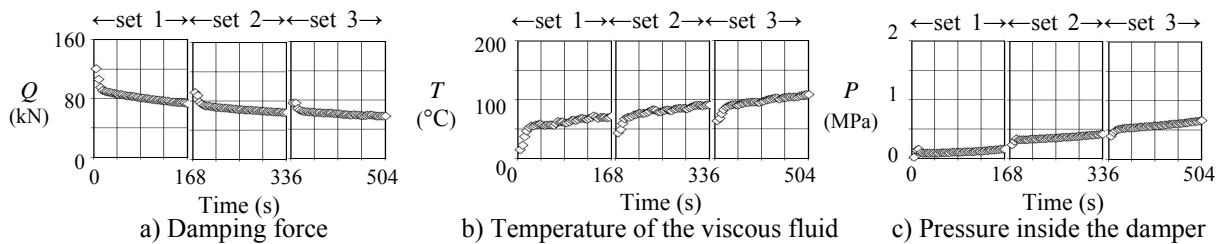


Figure 3.4. Result of multi-cyclic test for level 1 of RDT16

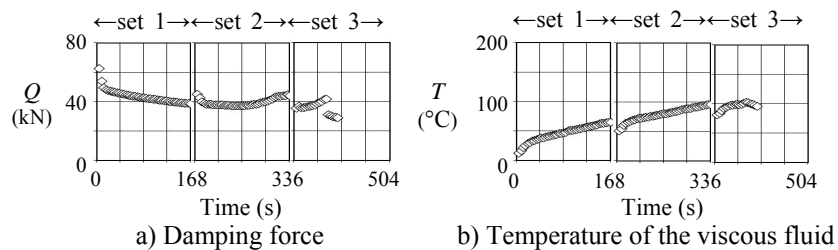


Figure 3.5. Result of multi-cyclic test for level 1 of RDT8

At 2nd set for level 1 of both RDT30 and RDT8, the damping force, which had been declining, started to rise again. At the same moment, it was observed that the pressure inside the damper RDT30 had considerably risen where the curve had become steep. At 3rd set for level 1 of RDT8, a seal portion of the temperature sensor was damaged, the viscous fluid leaked out (Fig. 3.6) and then the test was concluded.

Both mentioned phenomena are considered to be caused by the pressure rising. The former can be regarded as the serviceability limit state, where the threshold value is about 1.5 MPa. The latter can be regarded as the ultimate limit state in the scope of this investigation, where the threshold value exceeds 5.8MPa that was the maximum value measured in these tests (at level 1 of RDT30).

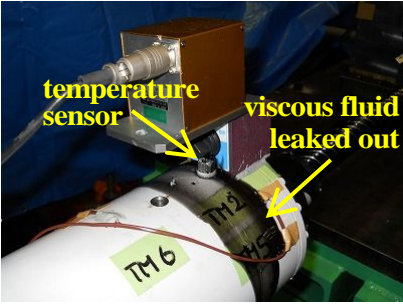


Figure 3.6. Leaking out of the viscous fluid

Fig. 3.7 shows the relations between damping force and displacement in the basic performance test of RDT16. The results shown here were those obtained before the test of each level, where temperature of viscous fluid had fallen enough then. The damping force values of these tests were compensated at 20 °C. Dynamic characteristics in these tests were equivalent, even after loading several sets of long period earthquake motions.

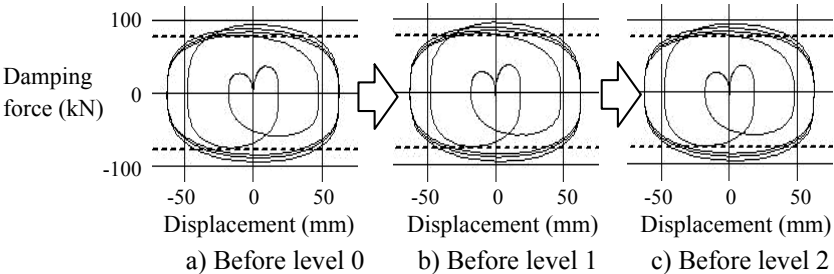


Figure 3.7. Results of the basic performance tests (RDT16)

Fig. 3.8 shows the ratio of the damping force obtained from the test of RDT16 to the value estimated by the conventional knowledge. The horizontal axis of the upper figure indicates the temperature of the viscous fluid, and that of the lower figure indicates the absorbed energy per viscous fluid volume. The scope of the conventional knowledge about the temperature of viscous fluid was up to 50 °C, and that about absorbed energy per viscous fluid volume was up to 1200J/cc. When the test conditions were set beyond these limits, the conventional knowledge could not estimate the damping force with enough accuracy.

Fig. 3.9 shows the relationship between the relative damping force Q/Q_0 and absorbed energy per viscous fluid volume E_d/V_v , where Q is the damping force of test results and Q_0 is the damping force corresponding to the initial temperature calculated using the conventional knowledge.

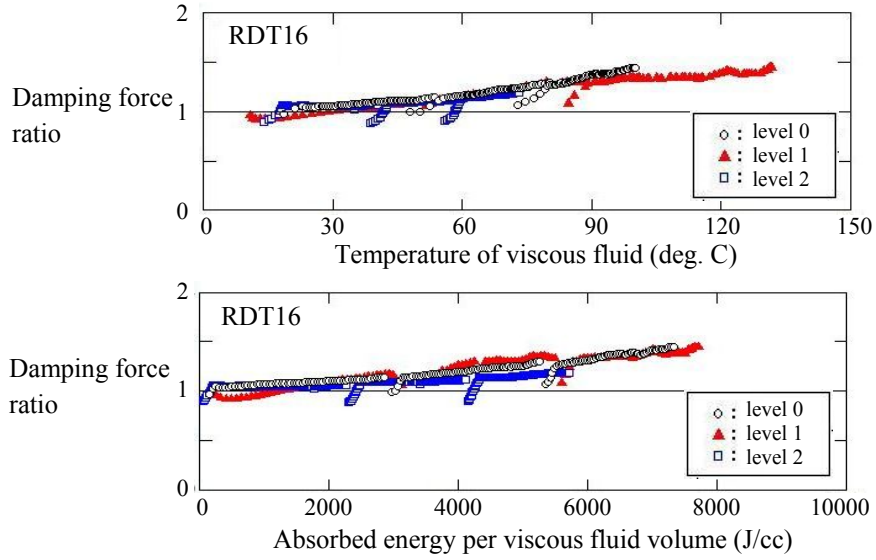


Figure 3.8. Comparison of damping force of test result and estimation by the conventional knowledge (RDT16)

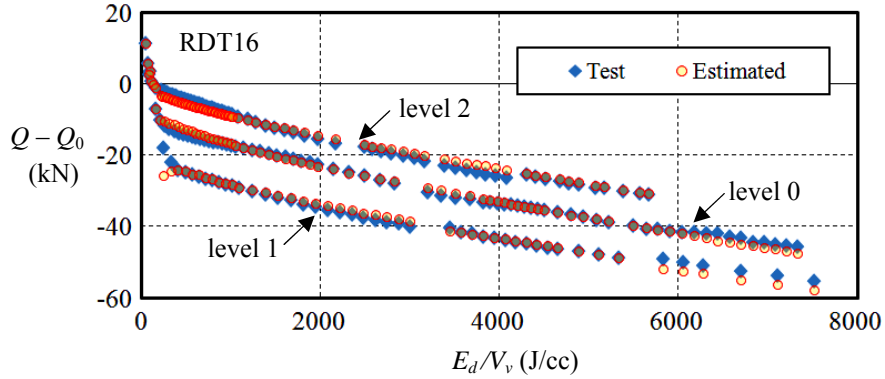


Figure 3.9. Comparison of damping force of test result and newly proposed estimation (RDT16)

The evaluation of the relative damping force $Q-Q_0$ is given by Eqn. 3.1 which includes E_d/V_v and its time increment $\Delta E_d/V_v$ as predictor variables. The values of coefficients a to e are listed in Table 3.4. As shown in Fig. 3.9, this equation can simulate the trend of fluctuation well. Fig. 3.10 shows the comparison of experimental and simulated damping force-displacement loop. The proposed equation properly illustrates the experimental result.

$$Q - Q_0 = a + b(E_d / V_v) + c(\Delta E_d / V_v) + d(\Delta E_d / V_v)^2 + e(E_d / V_v)^{0.5} (\Delta E_d / V_v)^{0.5} \quad (3.1)$$

Table 3.4. Coefficients of Eqn. 3.1

Specimen	E_d/V_v	a	b	c	d	e
RDT8	≤ 200	2.30	0.0769	2.23	-0.0350	-0.834
	200 to 300	linear interpolated				
	≥ 300	1.22	-0.00262	-0.224	-0.00508	-0.0121
RDT16	≤ 150	6.99	0.178	5.44	-0.0877	-2.16
	150 to 200	linear interpolated				
	≥ 200	0.134	-0.00345	0.395	-0.0572	-0.0914
RDT30	≤ 600	-25.5	0.0762	3.60	-0.0288	-1.15
	600 to 1000	linear interpolated				
	≥ 1000	-68.2	-0.00186	2.81	-0.0630	-0.0758

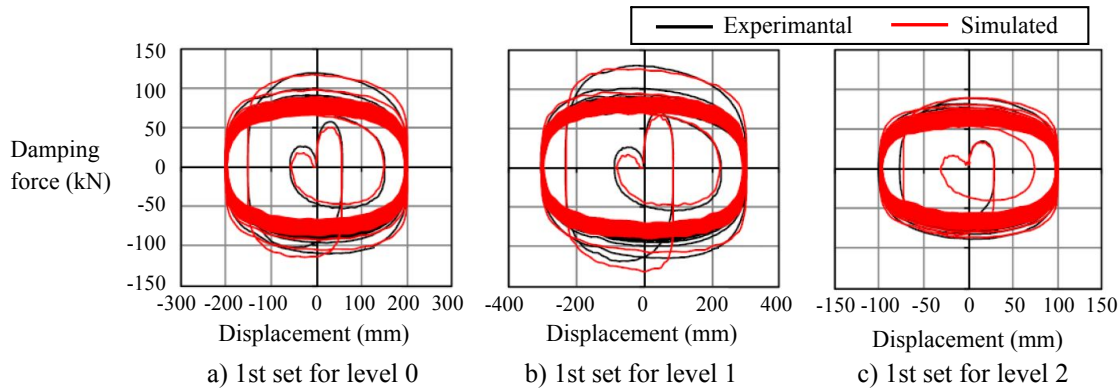


Figure 3.10. Comparison of experimental and simulated damping force-displacement loop (RDT16)

4. CONCLUSION

Based on the result of the investigation on oil dampers, through multi-cyclic loading test that gave the specimens total amount of forced displacement of 150m, following findings are drawn. 1) There was almost no change in the shape of the damping force and displacement loops. 2) There was a slight change in the amount of the absorbed energy, according to oil temperature rise. 3) Although the oil temperature exceeded the allowable value, i.e. 80 °C, leaking of oil out from seal was not observed.

The viscous dampers investigated have energy absorption capacity that can sustain at least 2 times of long period earthquake motions. The damping force declined continuously through the cyclic loading test. After the temperature of viscous fluid fell enough, the initial dynamic characteristics were recovered, even after loading of several sets of long period earthquake motions. A new evaluation formula that simulates properly the trend of the damping force was proposed.

ACKNOWLEDGEMENT

This paper describes a part of productions of the promotion project for building-standards maintenance "27-3 Examination about the safety verification method of the seismic isolated buildings against long-period ground motions" conducted by the Ministry of Land, Infrastructure, Transport and Tourism in the Heisei 22 fiscal year. Gratitude is respectfully expressed to the main committee (chairperson: Professor Haruyuki Kitamura of Tokyo University of Science), WG for testing of devices (chief examiner: Professor Mineo Takayama of Fukuoka University), WG for evaluation of response of buildings (chief examiner: Professor Takeshi Furuhashi of Nihon University) and all the persons concerned.

REFERENCES

- Japan Society of Seismic Isolation (2010). The Seismic Isolated Structure - From the Basis of Devices to the Design and the Construction - (in Japanese), Ohmsha, Tokyo, Japan.
- Shimizu, K., Kurino, H., Tagami, J., Hikita, M., Kotake, Y. and Suzuki, T. (2008). Heat Behavior of an Oil Damper against Energy Input (in Japanese). *Summeries of Technical Papers of Annual Meeting Architectural Institute of Japan 2008. Structures II*: 513-514.
- Shimizu Corporation, Kobori Research Complex Inc. and Japan Society of Seismic Isolation (2010). Examination on Maintenance of Standard for Seismic Isolated Structures (in Japanese). *The Report on the Promotion Project for Building-Standards Maintenance of Ministry of Land, Infrastructure, Transport and Tourism in the Heisei 21 Fiscal Year. No.12*:4.1-28-4.1-31.
- Ministry of Land, Infrastructure and Transport and Tourism (2004/2008) . An Attached Table of Building-Materials Verifition Document for AT Type Damping Devices with Amplification Mechanism – Gensui Koma – (in Japanese), **MVBR-0387, MVBR-0221 and MVBR-0222**